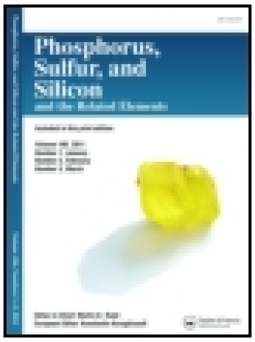

Phosphorus, Sulfur, and Silicon and the Related Elements

ISSN: 1042-6507 (Print) 1563-5325 (Online) Journal homepage: https://www.tandfonline.com/loi/gpss20

Research on hydroxyethyl ammonium O,O'-diphenyl dithiophosphate: Synthesis, characterization, surface activity and corrosion inhibition performance

Chuan Lai, Bin Xie & Xiaogang Guo

To cite this article: Chuan Lai, Bin Xie & Xiaogang Guo (2019): Research on hydroxyethyl ammonium O,O′-diphenyl dithiophosphate: Synthesis, characterization, surface activity and corrosion inhibition performance, Phosphorus, Sulfur, and Silicon and the Related Elements, DOI: 10.1080/10426507.2019.1639703

To link to this article: https://doi.org/10.1080/10426507.2019.1639703

PHOSPHORUS, SULFUR, AND SILICON AND THE RELATED ELEMENTS
https://doi.org/10.1080/10426507.2019.1639703

Research on hydroxyethyl ammonium O,O′-diphenyl dithiophosphate: Synthesis, characterization, surface activity and corrosion inhibition performance

Chuan Lai[a,b], Bin Xie[b], and Xiaogang Guo[c]

[a]School of Chemistry and Chemical Engineering, Sichuan University of Arts and Science, Dazhou, China; [b]School of Materials Science and Engineering, Sichuan University of Science and Engineering, Zigong, China; [c]College of Chemistry and Chemical Engineering, Yangtze Normal University, Chongqing, China

ABSTRACT

Hydroxyethyl ammonium O,O′-diphenyl dithiophosphate (HADD) acting as a surfactant and corrosion inhibitor was successfully synthesized and characterized by FT-IR, ^{1}H NMR and single crystal X-ray diffraction. Meanwhile, the inhibition effect of HADD on Q235 steel (Q235s) corrosion in H_2SO_4 solution was studied by weight loss and potentiodynamic polarization measurements. HADD turned out to be an effective corrosion inhibitor and the inhibition efficiency increased with HADD concentration increasing, and significantly decreased with increasing both temperature and H_2SO_4 concentration. Potentiodynamic polarization measurements indicated that HADD was a mixed-type inhibitor.

ARTICLE HISTORY
Received 27 April 2019
Accepted 30 June 2019

KEYWORDS
Synthesis; characterization; surface activity; corrosion inhibition

GRAPHICAL ABSTRACT

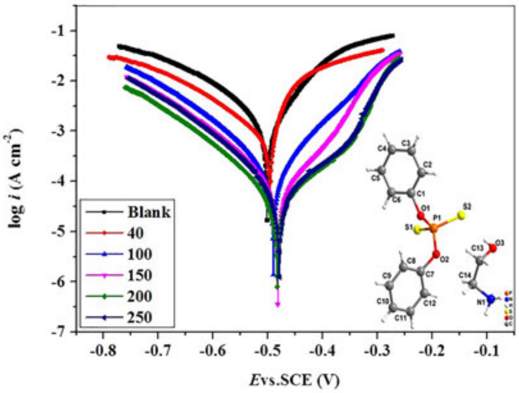

Introduction

Corrosion has become a common problem all over the world; wherever materials are used, there are corrosion problems emerging, and leading to major economic loss.[1,2] Among various types of corrosion, metal corrosion is extremely harmful. Based on metal corrosion problem, using corrosion inhibitors as an approach towards protection has become one of the most widely used methods due to its advantages of economy, high efficiency and universal scope.[3,4] Usually, corrosion inhibitors are a one-component compound or multicomponent chemicals that exist in the corrosive environment to prevent or slow down metal corrosion process. Especially in offshore oil and gas pipelines, chemical cleaning, petroleum products processing and other processes, more and more researchers have to admit that using corrosion inhibitors for corrosion prevention has become the most important method.[5–7]

With the development of corrosion inhibitor research and their applications in the field expanding, there are ample kinds of corrosion inhibitors to consider, among which organic corrosion inhibitors have obvious advantages as effective corrosion inhibitors. According to the relationships between inhibitors' structures and their corrosion inhibition performance, O,O′-diaryldithiophosphates and their derivatives are promising inhibitors because of the N, P and S atoms within the structures. The ionic compounds of O,O′-dialkyldithiophosphates diethyl ammonium such as (O,O′-bis(*p*-methoxyphenyl)dithiophosphate diethyl ammonium, O,O′-bis(4-chlorophenyl)dithiophosphate diethyl ammonium) and covalent compounds of O,O′-diaryldithiophosphates derivatives (S-benzyl-O,O′-bisphenyldithiophosphate, S-benzyl-O,O′-bisbenzyldithiophosphate, S-benzyl-O,O′-bis(2-phenylethyl)dithiophosphate, S-benzyl-O,O′-bis(4-methylphenyl)dithiophosphate, S-benzyl-O,O′-bis(2-naphthyl)

CONTACT Chuan Lai lc860801@163.com School of Chemistry and Chemical Engineering, Sichuan University of Arts and Science, Dazhou, 635000, China.
Color versions of one or more of the figures in the article can be found online at www.tandfonline.com/gpss.

Supplemental data for this article is available online at https://doi.org/10.1080/10426507.2019.1639703.

Table 1. Crystallographic data of HADD.

Compound	Hydroxyethyl ammonium O,O′-diphenyl dithiophosphate
Empirical formula	$C_{14}H_{18}NO_3PS_2$
Formula mass	343.38
Crystal system/Space group	Monoclinic, $P2_1/c$
a/Å	13.5330 (13)
b/Å	8.5681 (8)
c/Å	14.4688 (14)
α/°	90
β/°	103.5440 (10)
γ/°	90
V/Å^3	1631.0 (3)
Z	4
$D_{calcd.}$ (g cm^{-3})	1.398
μ (mm^{-1})	0.432
Crystal size (mm)	0.19 × 0.17 × 0.16
Color/Shape	Colorless, block
Temp (K)	100
Theta range for collection	2.78–25.00
Reflections collected	10886
Independent reflections	2863
Data/restraints/parameters	2863/4/190
Goodness of fit on F^2	1.026
Final R indices [$I > 2\sigma(I)$]	$R_1 = 0.0238$
R indices (all data)	$wR_2 = 0.0723$
Largest difference peak/hole	0.252, −0.296

$^{a}R_1 = \Sigma||F_o| - |F_c||/\Sigma|F_o|$, $wR_2 = [\Sigma w(F_o{}^2 - F_c{}^2)^2/\Sigma w(F_o{}^2)^2]^{1/2}$.

dithiophosphate, S-4-methylbenzyl-O,O′-bis(4-nitrophenyl) dithiophosphate, S-4-methylbenzyl-O,O′-bis(4-*tert*-butylphenyl)dithiophosphate, S-allyl-O,O′-bisphenyldithiophosphate, S-allyl-O,O′-bisbenzyldithiophosphate and S-allyl-O,O′-bis(2-phenylethyl) dithiophosphate) have been reported in our previous works as promising corrosion inhibitors.[4,6,8–11] According to our previous reports,[10,11] the inhibition efficiency for carbon steel in 0.5 M HCl with 100 mg L^{-1} concentration of O,O′-bis(p-methoxyphenyl)dithiophosphate diethyl ammonium at 300 K is 87.63%, and the inhibition efficiency for mild steel in 1.0 M HCl with 100 mg L^{-1} concentration of S-allyl-O,O′-bisphenyl dithiophosphate, S-allyl-O,O′-bisbenzyldithiophosphate and S-allyl-O,O′-bis(2-phenyl ethyl) dithiophosphate at 303 K are 82.75%, 98.74 and 93.26, respectively. Although these corrosion inhibitors showed good anti-corrosion properties, both covalent and ionic O,O′-dialkyldithiophosphates compounds all have low solubility in water and acid solution. In order to properly regulate the solubility of these inhibitors, hydroxyl groups are proposed to be introduced into the target O,O′-dialkyldithiophosphates, and the corresponding hydroxyethyl ammonium O,O′-diphenyldithiophosphate (HADD) would be synthesized and characterized. Meanwhile, the surface activity and corrosion inhibition performance would be evaluated in detail.

Results and discussion

Characterization of HADD

FT-IR and ^{1}H NMR

The FT-IR spectrum of HADD was presented in Figure S1 (Supplemental Materials). The peak at 3365.1 (s) cm^{-1} is attributable to the different hydroxyl groups (-OH) present in H_2O, and cationic group ([$H_3N^+CH_2CH_2OH$]) and those at 3008.0 (m) and 2937.1 (w) cm^{-1} belong to = C-H and -CH_2CH_2-, respectively. Peaks at wavenumbers of 1587.6 (s), 1484.9 (s) and 1450.7 (m) cm^{-1} represent C = C bands and those at 1207.5 (s), 1188.4 (s), 1162.4 (m), 1067.0 (m), 1004.8 (m) and 912.5 (s) cm^{-1} are assigned to (P)-O-C and (P-O-(C). At 879.0 (s), 770.4 (s) and 683.9 (s) cm^{-1} The peaks are attributable to S-C and PS_2.

According to ^{1}H NMR spectrum of HADD shown in Figure S2, the two triplets at 2.86 and 3.58 ppm are assigned to the CH_2CH_2 protons. Two singlet signals at 5.16 and 7.70 ppm are attributed to OH and $^+NH_3$ protons, respectively. Moreover, the phenyl proton signals exhibit one double of doublets at 7.26 ppm and two multiplets in the regions of 7.05–7.08 and 7.29–7.34 ppm. These results confirm that the structure of synthesized compound agrees with the structure of hydroxyethyl ammonium O,O′-diphenyl dithiophosphate.

Crystal structure of HADD

A colorless block single crystal with the size of 0.19 × 0.17 × 0.16 mm^3 was selected to determine the structure of HADD by single crystal X-ray diffraction. All crystal data were collected and summarized in Table 1. The crystal molecule structure and the 2D layer structure connected by the H-bonds of HADD shown in Figure 1 and Figure 2, respectively. The selected bond distances and bond angles of HADD listed in Table 2. Single-crystal X-ray analysis revealed that HADD shows a 0D molecule structure and crystallization in the monoclinic $P2_1/c$ space group. (CCDC 1908964)

The asymmetric unit is made up of the anionic group O,O′-diphenyldithiophosphate ($(PhO)_2P(S)S^-$) and the cationic group hydroxyethyl ammonium ($H_3N^+CH_2$ CH_2OH, Figure 1). The central P atom of the anionic group is coordinated by two O atoms from two different deprotonated phenol molecules and two S atoms. According to Table 2, the bond length of P (1) - O (1) (1.6254 (10) Å) is longer than the bond length of P (1) - O (2) (1.6163 (10) Å), and

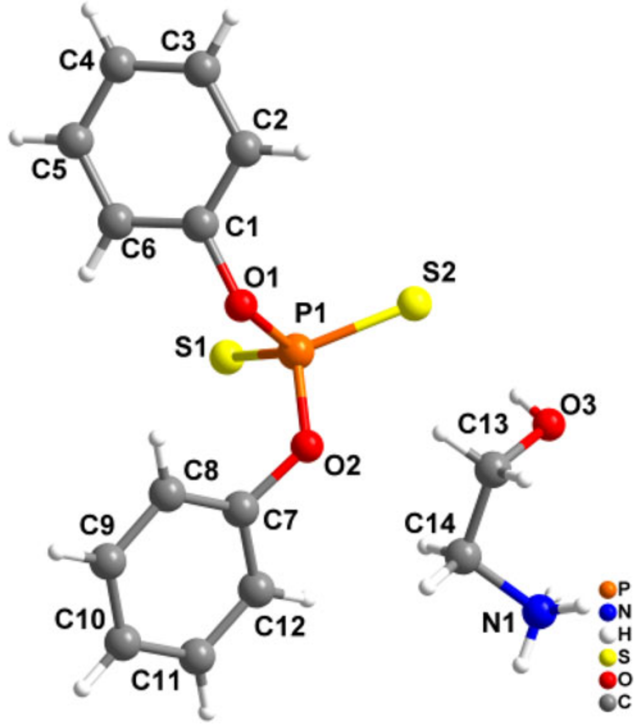

Figure 1. Crystal molecule structure of HADD.

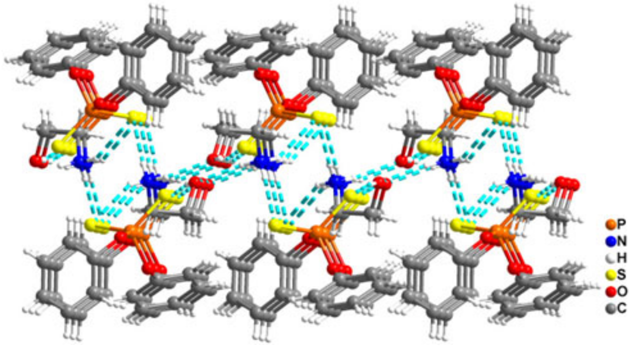

Figure 2. 2D layer structure of HADD.

Table 2. Selected bond distances (Å) and bond angles (°) of HADD.

Bond	Distances (Å)	Bond angles	Angles (°)
P (1) - O (2)	1.6163 (10)	O (2) - P (1) - O (1)	97.48 (5)
P (1) - O (1)	1.6254 (10)	O (2) - P (1) - S (2)	105.74 (4)
P (1) - S (2)	1.9632 (5)	O (1) - P (1) - S (2)	111.71 (4)
P (1) - S (1)	1.9676 (5)	O (2) - P (1) - S (1)	112.26 (4)
N (1) - C (14)	1.4953 (19)	O (1) - P (1) - S (1)	111.23 (4)
O (1) - C (1)	1.4054 (17)	S (2) - P (1) - S (1)	116.65 (2)
O (2) - C (8)	1.4077 (17)	C (1) - O (1) - P (1)	121.72 (9)
O (3) - C (13)	1.4289 (17)	C (8) - O (2) - P (1)	125.61 (9)
C (1) - C (6)	1.382 (2)	C (6) - C (1) - C (2)	121.79 (14)
O (3) - H (3B)	0.8264	C (6) - C (1) - O (1)	118.98 (13)
N (1)- H (1 WC)	0.8642	C (2) - C (1) - O (1)	119.18 (13)
N (1) - H (1 WB)	0.8626	C (18) - C(8) - O (2)	121.78 (13)
N (1) - H (1 WA)	0.8650	C (12) - C(8) - O (2)	116.43 (13)

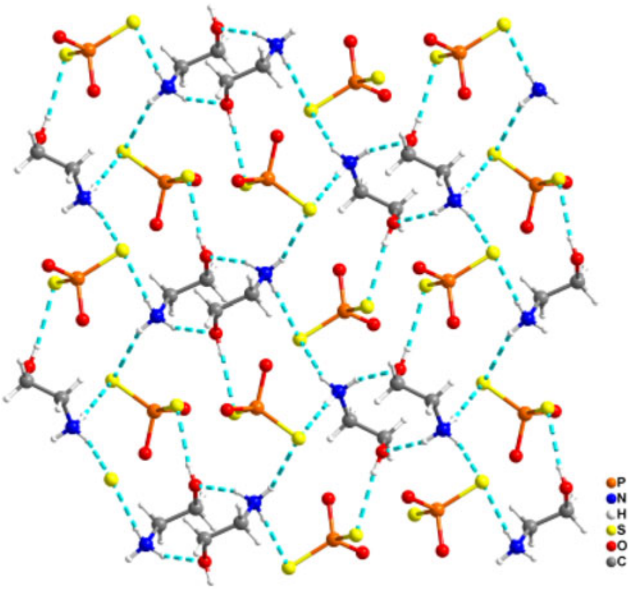

Figure 3. H-bonds between the molecule strctures in HADD.

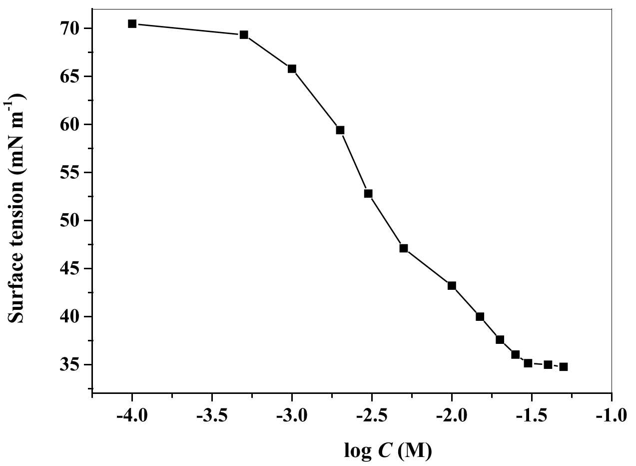

Figure 4. Variations in surface tension with HADD concentrations in double distilled water at 30 °C.

the bond length of P (1) - S (2) (1.9632 (5) Å) is shorter than the bond length of P (1) - S (1) (1.9676 (5) Å). The different bond lengths and different bond angles (O (2) - P (1) - O (1), O (2) - P (1) - S (2), O (1) - P (1) - S (2), O (2) - P (1) - S (1), O (1) - P (1) - S (1), S (2) - P (1) - S (1)) present that there is a distorted tetrahedral environment around P atom with two S atoms and two O atoms. Furthermore, the cationic group ($H_3N^+CH_2$ CH_2OH) on one hand helps to balance the charge, and on the other hand is formatting the H-bonds with the sulfur and oxygen atoms. In addition, the H-bonds [N1-H1A … O1 (2.827 Å); N1-H1B … O1 (2.011 Å and O3-H3 … S1 (2.457 Å)] between the anionic and cationic groups further connected the molecules in two 2D layer structures are presented in Figure 2 and Figure 3. And the 2D layer structures are packed into 3D network by the intermolecular interaction (Van der Waals force) between the 2D structures.

Surface active properties

Herein, the surface tension (γ) of HADD was measured for a range of concentrations above and below the critical micelle concentration (C_{cmc}). Figure 4 represents the plots of γ versus log C for HADD in double distilled water. An obvious decrease in surface tension is observed with increasing HADD concentration. This observation is recorded for

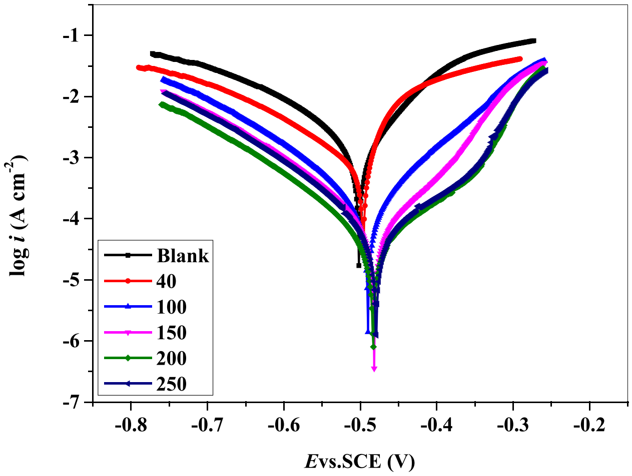

Figure 5. Potentiodynamic polarization curves for Q235s in 1.0 M H_2SO_4 with different concentrations of HADD at 30 °C.

Table 3. The polarization parameter of Q235s corrosion in 1.0 M H_2SO_4 with different concentrations of HADD at 30 °C.

c (mg L^{-1})	E (V)	ΔE (V)	i_{ccd} (μA cm^{-2})	β_a (mV dec^{-1})	β_c (mV dec^{-1})	IE_{PPM} (%)
0	−0.477	—	2887	132.57	152.86	—
40	−0.497	0.020	2448	45.18	131.68	42.81
100	−0.490	0.013	154.8	78.91	107.78	89.66
150	−0.482	0.005	68.41	91.85	107.14	97.63
200	−0.483	0.006	45.82	115.96	96.37	98.41
250	−0.479	0.002	43.27	122.03	97.20	98.50

HADD up to the C_{cmc}, beyond which no considerable changes are noticed, which is used to determine C_{cmc} of HADD. The C_{cmc} data, obtained from the break point in the γ - log C plots, was 27.386 mmol L^{-1} and the surface tension (γ_{cmc}) at C_{cmc} was 35.14 mN m^{-1}. Moreover, the maximum surface pressure (π_{cmc}) can be obtained from equation (1), where γ_0 (70.43 mN m^{-1}) was the surface tensions of double distilled water at 30 °C, and the calculated value of π_{cmc} was 35.29 mN m^{-1}. In addition, the γ - log C plots also provided information on area per molecule at air-water interface, effectiveness and surface excess concentration of surfactant ions of HADD.

$$\pi_{cmc} = \gamma_0 - \gamma_{cmc} \tag{1}$$

Potentiodynamic polarization measurement

Figure 5 presents the potentiodynamic polarization curves (Tafel curves) for Q235 in 1.0 M H_2SO_4 with various concentrations (0–250 mg L^{-1}) of HADD at 30 °C. The electrochemical parameters are listed in Table 3, including IE_{PPM} (inhibition efficiency), $i_{ccd(i)}$ (corrosion current density), E (vs SCE, V) (corrosion potential), β_c and β_a (cathodic and anodic Tafel slopes).

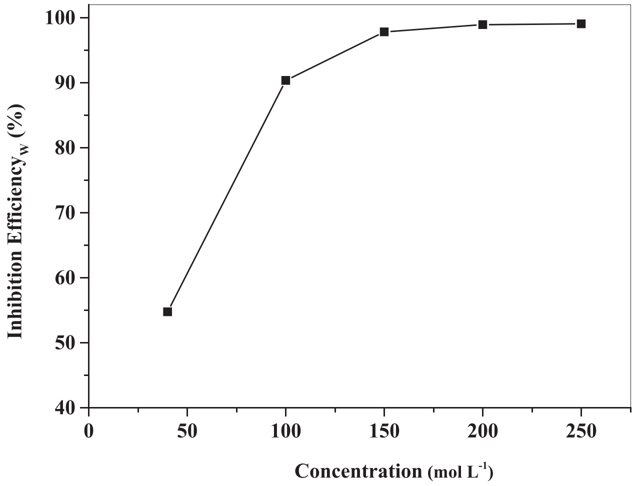

Figure 6. The effect of HADD concentration on inhibition efficiency (IE_W, %).

According to Figure 5 and Table 3, both anodic and cathodic curves shift to lower current densities with addition of HADD into the H_2SO_4 solution. In Table 3, the current density is much lower in the presence of HADD than that in the absence of HADD in H_2SO_4 solution, and decreases with increasing HADD concentration. When HADD concentration increases to 200 mg L^{-1}, the inhibition efficiency (IE_{PPM}, %) reaches to 98.41%. The increase of corrosion inhibition effect is due to the gradual adsorption of HADD on Q235s surface, resulting in a dense self-protective film, which also indicates that HADD can act as an effective inhibitor for Q235s in H_2SO_4 solution. Additionally, all corrosion potential exhibited in Table 3 shifts less than 10 mV ($\Delta E < 0.085$ V), which reveals that HADD is a mixed-type corrosion inhibitor.[11–16]

Weight loss measurement

Figure 6 shows the effect of HADD concentration on inhibition efficiency (IE_W, %) for Q235s in 1.0 M H_2SO_4 at 30 °C. Clearly, the inhibition efficiency increase with the HADD concentration increasing. As HADD concentration increases to 150 mg L^{-1}, the inhibition efficiency changes only slightly when HADD concentration further increases. The increase of inhibition efficiency is caused by the increasing of the coverage of HADD adsorbed on the surface of Q235s. With HADD concentration rises to 150 mg L^{-1} and 200 mg L^{-1}, the corresponding inhibition efficiency are 97.83% and 98.96%, which further demonstrates that HADD can act as an effective inhibitor.

Adsorption isotherms

According to the data of weight loss measurement from Figure 6, various isotherms including Freundlich, Temkin, Flory - Huggins, El - Awady and Langmuir adsorption isotherms were employed to confirm the reasonable adsorption isotherm for HADD on the Q235s surface. The five adsorption isotherms for HADD on the Q235s surface in 1.0 M H_2SO_4 showed in Figure 7a–e and Table 4. In Table 4, the R^2 increases from 0.934 (in Freundlich adsorption isotherm) to 0.995 (in Langmuir adsorption isotherm), revealing that the adsorption of HADD on Q235s surface obeys Langmuir adsorption isotherm showed in equations (2) and (3).[6,8,17–20]

$$\frac{c}{\theta} = \frac{1}{K} + c \tag{2}$$

$$\theta = \frac{v_0 - v_i}{v_0} \tag{3}$$

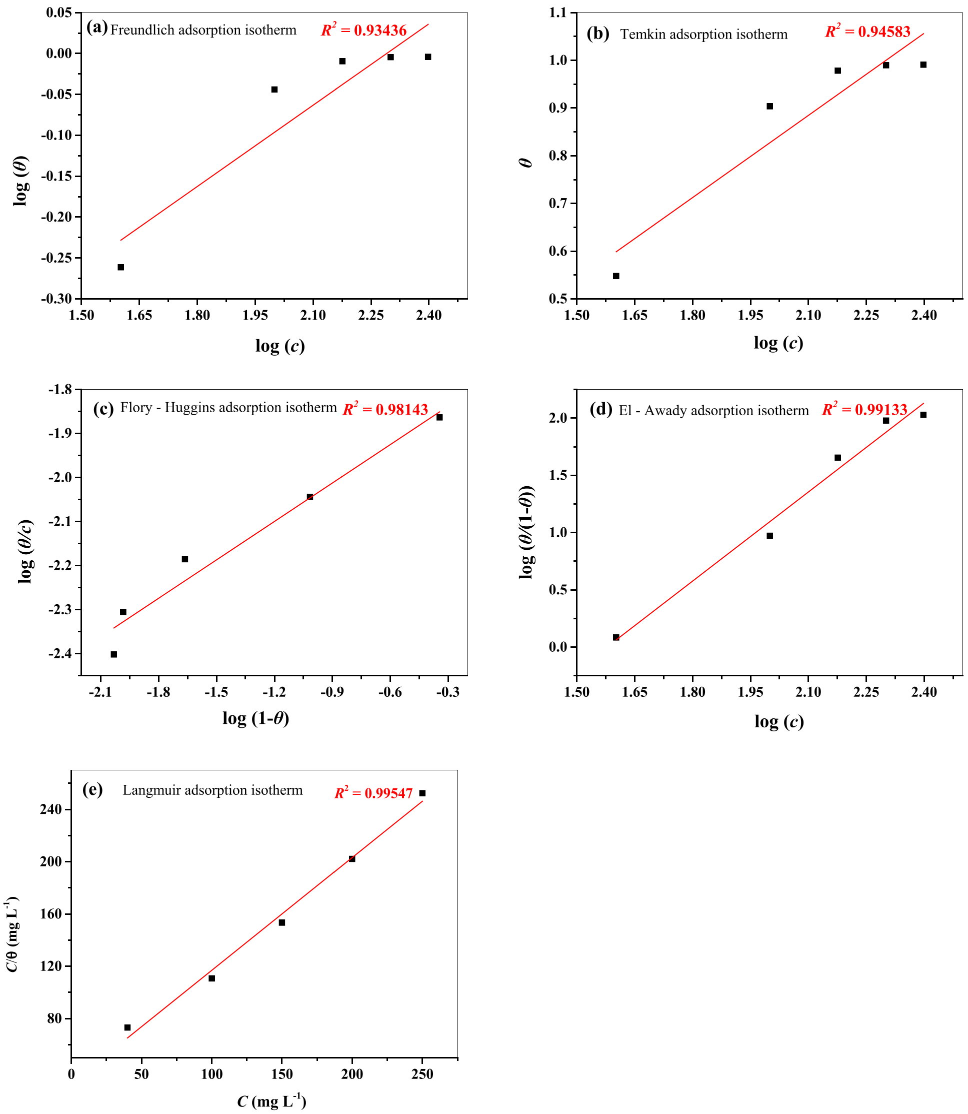

Figure 7. The plots of Freundlich (a), Temkin (b), Flory - Huggins (c), El - Awady (d) and Langmuir (e) adsorption isotherms for HADD on Q235 steel surface in 1.0 M H_2SO_4 at 30 °C.

$$\Delta G_a^0 = -RT\ln(55.5K_a) \tag{4}$$

$$K_a = M_{HADD} \times K \times 10^3 = \frac{343 \times 10^3}{30.6497} = 1.1191 \times 10^4 \ (\text{mol L}^{-1}) \tag{5}$$

Figure 7e shows the plots of c/θ versus c yield the straight lines. The strong correlation ($R^2 = 0.995$, see Figure 7e) suggests the adsorption of HADD on Q235's surface is conforming to Langmuir adsorption isotherm. Based on the fitted results, ΔG_a^0 (adsorption standard free energy) can be determined by equation (4), where the value of intercept ($1/K$, in equation (3)) is 30.6497 (mg L^{-1}) that can be used to calculate K_a shown in equation (5). The calculation is shown as follows $\Delta G_a^0 = -8.314 \times 303.15 \times \ln(55.5 \times 1.1191 \times 10^4) = -33.62$ (kJ mol^{-1}), where the ΔG_a^0 for Q235s corrosion in 1.0 M H_2SO_4 with different concentrations of HADD at 30 °C is -33.62 kJ mol^{-1} (> -40.00 kJ mol^{-1}) which also indicates that the adsorption processes of HADD on Q235s surface belong to mixed adsorption involving both physisorption and chemisorption.[7,9,21–23]

Effect factors

In this work, the single factor experiment was employed to study the effect of temperature (T, °C), H_2SO_4 concentration (C_H, M) and immersion time (t, h) on inhibition efficiency (IE_W, %), and the relative results were listed in Table 5. Obviously, all the factors involving temperature, H_2SO_4 concentration and immersion time can affect the corrosion inhibition of Q235s in H_2SO_4 solution, among which the temperature and H_2SO_4 concentration have particularly significant effects on inhibition efficiency, while the immersion time has a small effect. It is obviously seen that with the temperature and H_2SO_4 concentration increasing, the inhibition efficiency decreased sharply. When the temperature increased from 10 °C to 80 °C, the inhibition efficiency decreased from 99.76% to 28.77% for Q235s in 1.0 M H_2SO_4, and the inhibition efficiency decreased from 99.47% to 78.36% for Q235s in H_2SO_4 solution at 30 °C by H_2SO_4 concentration increased from 0.1 M to 4.0 M. Furthermore, the inhibition efficiency decreased slightly as immersion time increasing, when immersion time decreased from 24 h to 192 h for Q235s in 1.0 M H_2SO_4 at 30 °C, the inhibition efficiency only decreased from 97.33% to 95.84%. This slight decrease (1.49%) is attributed to the hydrolysis of HADD in H_2SO_4 solution presented in Figure 8.

Experimental

Materials

All analytically pure chemicals including toluene, phenol, phosphorus pentasulphide, ethanolamine and sulfuric acid (98%) used to synthesize target compound and prepare aggressive medium were not further purified before used. The working electrode and test samples were prepared by Q235 steel (Q235s) with the chemical compositions (wt.%) of Mn (0.531), Si (0.270), C (0.187), P (<0.040), S (<0.045) and Fe (Bal.).

Moreover, the synthesized inhibitor was confirmed by Fourier Transform infrared spectrometer (FT-IR, Nicolet iS10, USA) and nuclear magnetic resonance (NMR, Bruker av400, Germany). Crystal data were collected on a diffractometer (SMART APEX-II, Bruker-AXS, Germany). Meanwhile, the surface tension was measured by surface Tensiometer (A101Plus, KINO Industry Co., Ltd, USA), and the electrochemical tests were employed by electrochemical workstation (CHI 760E, China).

Table 4. Fitting results of different adsorption isotherms for HADD on Q235s in 1.0 M H_2SO_4 at 30 °C.

Number	Isotherms	Pearson's R^2	Equation ($y = a + b*x$)
(a)	Freundlich	0.93436	$y = 0.33162 * x - 0.75961$
(b)	Temkin	0.94583	$y = 0.57444 * x - 0.32171$
(c)	Flory - Huggins	0.98143	$y = 0.29087 * x - 1.75068$
(d)	El - Awady	0.98933	$y = 2.59613 * x - 4.09702$
(e)	Langmuir	0.99547	$y = 0.88247 * x + 30.6497$

Table 5. Effect of temperature (T, °C), H_2SO_4 concentration (C_H, M) and immersion time (t, h) on inhibition efficiency for Q235s in H_2SO_4 solution by weight loss measurements.

Temperature (T, °C)	IE_{WLM} (%)	H_2SO_4 concentration (C_H, M)	IE_{WLM} (%)	immersion time (t, h)	IE_{WLM} (%)
10	99.76	0.1	99.47	0	97.83
30	97.83	0.5	98.97	24	97.33
50	83.30	1.0	97.83	48	96.41
70	62.47	2.0	91.44	96	96.37
80	28.77	4.0	78.36	192	95.84

Synthesis and characterization of HADD

Synthesis

According to the synthetic method described in our previous works,[4,6,8] hydroxyethyl ammonium O,O′-diphenyl dithiophosphate ($[(PhO)_2P(S)S^-][H_3N^+ CH_2CH_2OH]$, HADD) as a surfactant and corrosion inhibitor was prepared by the reaction of phosphorus pentasulfide with phenol and ethanolamine using toluene as the solvent under the reflux condition. The synthetic route and corresponding chemical structures of $(PhO)_2P(S)SH$ and $[(PhO)_2P(S)S^-][H_3N^+CH_2CH_2OH]$) are presented in Figure 9.

Characterization

FT-IR (KBr, cm^{-1}): 3365.1 (s), 3008.0 (m), 2937.1 (w), 1587.6 (s), 1484.9 (s), 1450.7 (m), 1207.5 (s), 1188.4 (s), 1162.4 (m), 1067.0 (m), 1004.8(m), 912.5 (s), 879.0 (s), 770.4 (s), 683.9 (s). ^{1}H NMR (400 MHz, DMSO): $\delta = 2.86$ (t, $J = 5.2$ Hz, 2 H, $^+NH_3CH_2$), 3.58 (t, $J = 5.2$ Hz, 2 H, $HOCH_2$), 5.16 (s, 1 H, OH), 7.05–7.08 (m, 2 H, *o*-Ph*H*), 7.26 (dd, $J = 6.1$, 5.1 Hz, 2 H, *p*-Ph*H*), 7.29–7.34 (m, 4 H, *m*-Ph*H*), 7.70 (s, 3 H, $^+NH_3$) ppm.

Surface tension measurement

Surface tension was measured for different concentrations of HADD dissolved in double distilled water with a surface Tensiometer (A101Plus, KINO Industry Co., Ltd, USA). At 30 °C, the double distilled water was used to prepare test solutions with a surface tension 70.43 mN m^{-1}.

Weight loss measurement

Weight loss measurements to evaluate the corrosion inhibition performance of steel in acidic solutions were described

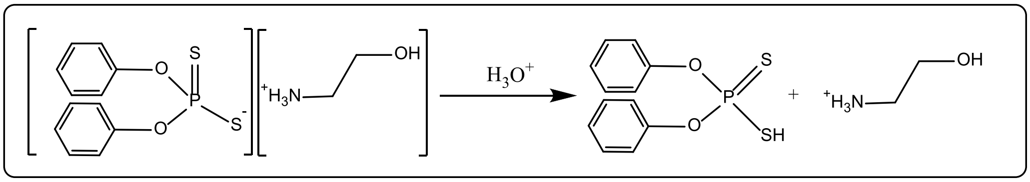

Figure 8. The hydrolysis schematic of HADD in H_2SO_4 solution.

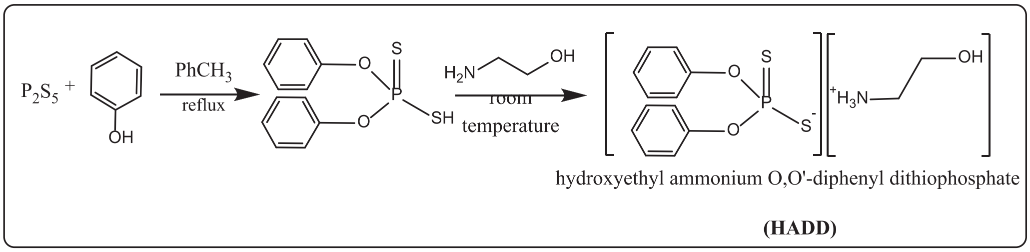

Figure 9. Synthetic process of hydroxyethyl ammonium O,O′-diphenyl dithiophosphate (HADD).

in our previous work and other researchers.[10,23–26] The corrosion rate (v) and inhibition efficiency (IE_{WLM}, %) were obtained from equations (1) and (2), respectively.

$$v_i = \frac{m_0 - m_\mathrm{i}}{St} \tag{6}$$

$$IE_{\mathrm{WLM}}\ (\%) = \frac{v_0 - v_i}{v_0} \times 100 \tag{7}$$

Potentiodynamic polarization measurement

According to potentiodynamic polarization measurement, the potential sweep rate was set as 0.5 mV s^{-1}. The inhibition efficiency (IE_{PPM}, %) was calculated by equation (8).[27–30]

$$IE_{\mathrm{PPM}}\ (\%) = \frac{i_{\mathrm{ccd(0)}} - i_{\mathrm{ccd(i)}}}{i_{\mathrm{ccd(0)}}} \times 100 \tag{8}$$

Conclusions

In conclusion, the new compound of hydroxyethyl ammonium O,O′-diphenyl dithiophosphate (HADD) acting as the anionic surfactant and corrosion inhibitor was facilely synthesized and characterized by FT-IR, ^{1}H NMR and single crystal X-ray diffraction. Study results indicate that HADD can be act as an excellent surfactant and the C_{cmc} is 27.386 mmol L^{-1}. Weight loss measurement and potentiodynamic polarization measurement results present that HADD is an effective corrosion inhibitor, and the inhibition efficiency increased with HADD concentration increasing and significantly decreased with both temperature and H_2SO_4 concentration increasing. HADD turns out to be a mixed-type effective corrosion inhibitor, which obeys Langmuir isotherm being adsorpted on Q235s surface, and it is a mixed adsorption involving both the physisorption and chemisorption mechanism.

Disclosure statement

No potential conflict of interest was reported by the authors.

Funding

This project is supported financially by the opening project of Key Laboratories of Fine Chemicals and Surfactants in Sichuan Provincial Universities (2018JXZ01, 2016JXZ03), the projects of Sichuan University of Arts and Science (2018SCL001Z, 2018KC005Z), the program of Science and Technology Department of Sichuan Province (2018JY0061), the program of Education Department of Sichuan Province (18CZ0038), and the project of Dazhou City (18ZDYF0008, 18ZDYF0009).

ORCID

Chuan Lai http://orcid.org/0000-0001-6213-4598

References

[1] AfifAnaee, R.; Tomi, I. H.-R.; Abdulmajeed, M.-H.; Naser, S.-A.; Kathem, M.-M. Expired Etoricoxib as a Corrosion Inhibitor for Steel in Acidic Solution. *J. Mol. Liq.* **2019**, *279*, 594–602. DOI: 10.1016/j.molliq.2019.01.169.

[2] Obot, I.-B.; Onyeachu, I.-B.; Wazzan, N.; Al-Amri, A.-H. Theoretical and Experimental Investigation of Two Alkyl Carboxylates as Corrosion Inhibitors for Steel in Acidic Medium. *J. Mol. Liq.* **2019**, *279*, 190–207. DOI: 10.1016/j.molliq.2019.01.116.

[3] Monticelli, C.; Balbo, A.; Esvan, J.; Chiavari, C.; Martini, C.; Zanotto, F.; Marvelli, L.; Robbiola, L. Evaluation of 2-(Salicylideneimino) Thiophenol and Other Schiff Bases as Bronze Corrosion Inhibitors by Electrochemical Techniques and Surface Analysis. *Corros. Sci.* **2019**, *148*, 144–158. DOI: 10.1016/j.corsci.2018.12.017.

[4] Lai, C.; Guo, X.-G.; Wei, J.; Xie, B.; Zou, L.-L.; Li, X.-L.; Chen, Z.-X.; Wang, C.-M. Investigation on Two Compounds of O,O′-Dithiophosphate Derivatives as Corrosion Inhibitors for Q235 Steel in Hydrochloric Acid Solution. *Open Chem.* **2017**, *15*, 263–271. DOI: 10.1515/chem-2017-0034.

[5] Fernandes, C.-M.; Alvarez, L.-X.; Santos, N.-E.; Barrios, A. C.-M.; Ponzio, E.-A. Green Synthesis of 1-Benzyl-4-Phenyl-1H-1,2,3-Triazole, Its Application as Corrosion Inhibitor for Mild Steel in Acidic Medium and New Approach of Classical Electrochemical Analyses. *Corros. Sci.* **2019**, *149*, 185–194. DOI: 10.1016/j.corsci.2019.01.019.

[6] Su, X.-L.; Lai, C.; Peng, L.-C.; Zhu, H.; Zhou, L.-S.; Zhang, L.; Liu, X.-Q.; Zhang, W. A Dialkyldithiophosphate Derivative as Mild Steel Corrosion Inhibitor in Sulfuric Acid Solution. *Int. J. Electrochem. Sci.* **2016**, *11*, 4828–4839. DOI: 10.20964/2016.07.101.

[7] Tan, B.; Zhang, S.-T.; Liu, H.-Y.; Guo, Y. W.; Qiang, Y.-J.; Li, W.-P.; Guo, L.; Xu, C. L.; Chen, S.-J. Corrosion Inhibition of X65 Steel in Sulfuric Acid by Two Food Flavorants 2-Isobutylthiazole and 1-(1,3-Thiazol-2-yl) Ethanone as the Green Environmental Corrosion Inhibitors: Combination of Experimental and Theoretical Researches. *J. Colloid Interf. Sci.* **2019**, *538*, 519–529. DOI: 10.1016/j.jcis.2018.12.020.

[8] Wang, C.-D.; Lai, C.; Xie, B.; Guo, X.-G.; Fu, D.; Li, B.; Zhu, S.-S. Corrosion Inhibition of Mild Steel in HCl Medium by S-benzyl-O,O′-Bis(2-Naphthyl) Dithiophosphate with Ultra-Long Lifespan. *Results Phys.* **2018**, *10*, 558–567. DOI: 10.1016/j.rinp.2018.07.002.

[9] Lai, C.; Wei, J.; Guo, X.-G.; Xie, B.; Zou, L.-K.; Ma, X.; Zhu, S.-S.; Chen, L.; Luo, G. B. Study on S-4-methylbenzyl-O,O′-Dithiophosphates as Corrosion Inhibitors for Q235 Steel in HCl Solution. *Int. J. Electrochem. Sci.* **2017**, *12*, 10457–10470. DOI: 10.20964/2017.11.16.

[10] Lai, C.; Xie, B.; Zou, L.-K.; Zheng, X.-W.; Ma, X.; Zhu, S.-S. Adsorption and Corrosion Inhibition of Mild Steel in Hydrochloric Acid Solution by S-allyl-O,O′-Dialkyldithiophosphates. *Results Phys.* **2017**, *7*, 3434–3443. DOI: 10.1016/j.rinp.2017.09.012.

[11] Lai, C.; Xie, B.; Liu, C.-L.; Gou, W.; Zhou, L.-S.; Su, X.-L.; Zou, L.-L. A Study of N,N-Diethylammonium O,O′-di(p-Methoxyphenyl)Dithiophosphate as New Corrosion Inhibitor for Carbon Steel in Hydrochloric Acid Solution. *Inter. J. Corros.* **2016**, *2016*, 1–8. DOI: 10.1155/2016/1907634.

[12] Zhang, G. A.; Hou, X. M.; Hou, B. S.; Liu, H. F. Benzimidazole Derivatives as Novel Inhibitors for the Corrosion of Mild Steel in Acidic Solution: Experimental and Theoretical Studies. *J. Mol. Liq.* **2019**, *278*, 413–427. DOI: 10.1016/j.molliq.2019.01.060.

[13] Rabizadeh, T.; Asl, S.-K. Casein as a Natural Protein to Inhibit the Corrosion of Mild Steel in HCl Solution. *J. Mol. Liq.* **2019**, *276*, 694–704. DOI: 10.1016/j.molliq.2018.11.162.

[14] Pohrebova, I.-S.; Pylypenko, T.-M. Inhibitors for Acid Corrosion of Metals Based on Quaternary Pyridinium Salts Containing Carbonyl Groups. *Mater. Today: Proc.* **2019**, *6*, 192–201. DOI: 10.1016/j.matpr.2018.10.094.

[15] Luo, X.-H.; Ci, C.-G.; Li, J.; Lin, K.-D.; Du, S.; Zhang, H.-X.; Li, X.-B.; Cheng, Y.-F.; Zang, J.-C.; Liu, Y.-L. 4-aminoazobenzene Modified Natural Glucomannan as a Green Eco-Friendly Inhibitor for the Mild Steel in 0.5 M HCl Solution. *Corros. Sci.* **2019**, *151*, 132–142. DOI: 10.1016/j.corsci.2019.02.027.

[16] Murmu, M.; Saha, S.-K.; Murmu, N.-C.; Banerjee, P. Effect of Stereo Chemical Conformation into the Corrosion Inhibitive Behaviour of Double Azomethine Based Schiff Bases on Mild Steel Surface in 1 Mol L^{-1} HCl Medium: An Experimental, Density Functional Theory and Molecular Dynamics Simulation Study. *Corros. Sci.* **2019**, *146*, 134–151. DOI: 10.1016/j.corsci.2018.10.002.

[17] Ituen, E.; Akaranta, O.; James, A. Corrosion Inhibition Characteristics of 2-[(E)-[5-Methoxy-1-[4-(Trifluoromethyl)Phenyl] Pentylidene]Amino]Oxyethanamine on Steel in Simulated Oilfield Acidizing Solution. *J. King Saud Univ. Eng. Sci.* **2019**, *31*, 191–199. DOI: 10.1016/j.jksues.2017.07.002.

[18] Popoola, L.-T. Progress on Pharmaceutical Drugs, Plant Extracts and Ionic Liquids as Corrosion Inhibitors. *Heliyon* **2019**, *5*, e01143. DOI: 10.1016/j.heliyon.2019.e01143.

[19] Shaban, S.-M.; Aiad, I.; Moustafa, A.-H.; Aljoboury, O.-H. Some Alginates Polymeric Cationic Surfactants; Surface Study and Their Evaluation as Biocide and Corrosion Inhibitors. *J. Mol. Liq.* **2019**, *276*, 164–176. DOI: 10.1016/j.molliq.2018.10.017.

[20] Vasyliev, G.; Vorobiova, V. Rape Grist Extract (Brassica Napus) as a Green Corrosion Inhibitor for Water Systems. *Mater. Today: Proc.* **2019**, *6*, 178–186. DOI: 10.1016/j.matpr.2018.10.092.

[21] Gong, W.-N.; Yin, X.-S.; Liu, Y.; Chen, Y.; Yang, W.-Z. 2-Amino-4-(4-Methoxyphen yl)-Thiazole as a Novel Corrosion Inhibitor for Mild Steel in Acidic Medium. *Prog. Org. Coat.* **2019**, *126*, 150–161. DOI: 10.1016/j.porgcoat.2018.10.001.

[22] Zhang, Q.-H.; Hou, B.-S.; Xu, N.; Liu, H.-F.; Zhang, G.-A. Two Novel Thiadiazole Derivatives as Highly Efficient Inhibitors for the Corrosion of Mild Steel in the CO_2-Saturated Oilfield Produced Water. *J. Taiwan Inst. Chem. Eng.* **2019**, *96*, 588–598. DOI: 10.1016/j.jtice.2018.11.022.

[23] Sanaei, Z.; Ramezanzadeh, M.; Bahlakeh, G.; Ramezanzadeh, B. Use of Rosa Canina Fruit Extract as a Green Corrosion Inhibitor for Mild Steel in 1M HCl Solution: A Complementary Experimental, Molecular Dynamics and Quantum Mechanics Investigation. *J. Ind. Eng. Chem.* **2019**, *69*, 18–31. DOI: 10.1016/j.jiec.2018.09.013.

[24] Verma, D.-K.; Ebenso, E.-E.; Quraishi, M.-A.; Verma, C. Gravimetric, Electrochemical Surface and Density Functional Theory Study of Acetohydroxamic and Benzohydroxamic Acids as Corrosion Inhibitors for Copper in 1 M HCl. *Results Phys.* **2019**, *13*, 102194. DOI: 10.1016/j.rinp.2019.102194.

[25] Obot, I.-B.; Umoren, S.-A.; Ankah, N.-K. Pyrazine Derivatives as Green Oil Field Corrosion Inhibitors for Steel. *J. Mol. Liq.* **2019**, *277*, 749–761. DOI: 10.1016/j.molliq.2018.12.108.

[26] Mobin, M.; Basik, M.; Aslam, J. Pineapple Stem Extract (Bromelain) as an Environmental Friendly Novel Corrosion Inhibitor for Low Carbon Steel in 1 M HCl. *Measurement* **2019**, *134*, 595–605. DOI: 10.1016/j.measurement.2018.11.003.

[27] Dehghani, A.; Bahlakeh, G.; Ramezanzadeh, B.; Ramezanzadeh, M. Potential of Borage Flower Aqueous Extract as an Environmentally Sustainable Corrosion Inhibitor for Acid Corrosion of Mild Steel: Electrochemical and Theoretical Studies. *J. Mol. Liq.* **2019**, *277*, 895–911. DOI: 10.1016/j.molliq.2019.01.008.

[28] Javidi, M.; Chamanfar, R.; Bekhrad, S. Investigation on the Efficiency of Corrosion Inhibitor in CO2 Corrosion of Carbon Steel in the Presence of Iron Carbonate Scale. *J. Nat. Gas Sci. Eng.* **2019**, *61*, 197–205. DOI: 10.1016/j.jngse.2018.11.017.

[29] Likhanova, N.-V.; Arellanes-Lozada, P.; Olivares-Xometl, O.; Hernández-Cocoletzi, H.; Lijanova, I.-V.; Arriola-Morales, J.; Castellanos-Aguila, J.-E. Effect of Organic Anions on Ionic Liquids as Corrosion Inhibitors of Steel in Sulfuric Acid Solution. *J. Mol. Liq.* **2019**, *279*, 267–278. DOI: 10.1016/j.molliq.2019.01.126.

[30] Macedo, R. G. M.-A.; Marques, N.-N.; Tonholo, J.; Balaban, R.-C. Water-Soluble Carboxymethylchitosan Used as Corrosion Inhibitor for Carbon Steel in Saline Medium. *Carbohyd. Polym.* **2019**, *205*, 371–376. DOI: 10.1016/j.carbpol.2018.10.081.